IEEE 2012 Nuclear Science Symposium and Medical Imaging Conference,
Anaheim, California, USA, October 29 –November 3, 2012.

LA-UR-11-06426

MCNP6 ENHANCEMENTS OF DELAYED-PARTICLE PRODUCTION

Gregg W. McKinney
Los Alamos National Laboratory
P.O. Box 1663, MS C921, Los Alamos, NM 87545
gwm@lanl.gov

ABSTRACT

Over the last decade, there has been an increased interest in the production of delayed-particle signatures from neutron and photon interactions with matter. To address this interest, various radiation transport codes have developed a wide range of delayed-particle physics packages. With the recent merger of the Monte Carlo transport codes MCNP5 and MCNPX, MCNP6 inherited the comprehensive model-based delayed-particle production capabilities developed in MCNPX over the last few years. An integral part of this capability consists of the depletion code CINDER90 which was incorporated into MCNPX in 2004. During this last year, significant improvements have been made to the MCNP6 physics and algorithms associated with delayed-particle production, including the development of a delayed-beta capability, an algorithm enhancement for the delayed-neutron treatment, and a database enhancement for delayed-gamma emission. The delayed-beta feature represents an important component in modeling background signals produced by active interrogation sources. Combined, these improvements provide MCNP6 with a flexible state-of-the-art physics package for generating high-fidelity signatures from fission and activation. This paper provides details of these enhancements and presents results for a variety of fission and activation examples.

Key Words: Beta decay, delayed neutron, delayed gamma, delayed beta, delayed-particle production, Monte Carlo transport.

1. INTRODUCTION

Over the last decade, there has been an increased interest in the production of delayed-particle signatures from neutron and photon interactions with matter. To address this interest, various radiation transport codes have developed a wide range of delayed-particle physics packages [1,2,3]. Likewise, in early 2004 [4], Los Alamos National Laboratory (LANL) began development of such a physics package with the incorporation of the depletion code CINDER90 [5] within the Monte Carlo radiation transport code MCNPX [6]. Over the next few years, various improvements [7,8,9] were made to this capability, which were included in the 2.6.0 public release of MCNPX in 2008 [10]. With the recent merger of MCNP5 [11] and MCNPX in 2010, MCNP6 [12] inherited this comprehensive model-based delayed-particle production capability. Finally, during this last year, an additional set of significant improvements were made to the MCNP6 delayed-particle physics and algorithms. These improvements are the subject of this paper and include: development of a delayed-beta capability, an algorithm enhancement for the delayed-neutron treatment, and a database enhancement for delayed-gamma emission.

2. BACKGROUND

There are four major components to a predictive delayed-particle physics package: (1) a valid sampling of the precursors (or interaction residuals), (2) a meticulous and robust decay-chain methodology, (3) a comprehensive and accurate database of decay data, and (4) a precise and efficient sampling algorithm. Each of these is discussed briefly in the following paragraphs.

2.1. Nuclear Interaction Residuals

The determination of residuals from nuclear interactions is not as straightforward as one might hope. In fact, even today most radiation transport codes don't compute or provide information about transmuted nuclei, especially when an interaction is treated by "library" physics (i.e., the physics is encapsulated in data files that contain cross sections, lists of reactions, distributions, etc.). Traditionally, residual distributions were omitted from such data libraries, as the need for them was somewhat rare. In the following discussion, the MCNP6 transport physics is categorized into two groups: library-based physics and model-based physics. The former is typically utilized for low-energy transport (E<~100 MeV), while the latter tends to be invoked at high energies. One significant advantage of most model-based physics packages is that they provide very accurate identification of residuals. On the other hand, the lack of residual identification for library-based transport presents a challenge for delayed-particle production. In MCNP6, this was overcome for neutron interactions in two ways: (a) use of high-fidelity fission-product distributions for fission reactions, and (b) use of a simple, but effective, conversion algorithm for non-fission reactions (or activation, for ease of discussion). The latter approach involves creating a table that lists all possible library reactions and their related nucleonic adjustments (MCNP6 reaction identifiers are taken from the ENDF/B-VII [13] standard). For neutron-induced fission, MCNP6 uses three yield sets (thermal, fast, high energy) developed by England and Rider [14], and for photon-induced fission, MCNP6 uses yields produced by the GEF code [15].

2.2. Decay-Chain Methodology

Although CINDER90 is best known for its ability to perform accurate depletion analyses, a small subset of this capability, namely the decay chain constructor, has proven invaluable in the MCNP6 delayed-particle physics package. Details regarding this on-the-fly technique for computing decay-chain isotopics can be found in reference 5. Since these isotopics are normalized to a single precursor atom, they are used in the delayed-particle physics package as isotopic emission probabilities (see reference 7 for additional information).

2.3. Decay Data

First, it should be noted that a library-based approach to delayed-neutron emission has existed in MCNP/MCNPX since ~2001. This Keepin data [16] consisted of spectra that were condensed into six time groups and incorporated into the ACE (A Compact ENDF) libraries of several actinides. On the other hand, our more recent MCNPX/MCNP6 model-based physics package has accrued its delayed-particle emission data from a variety of sources throughout its 8 years of development. Early on, this data consisted of a comprehensive set of bin-wise (25 bins) gamma-

emission spectra and a single neutron-emission spectrum. The gamma spectra were based principally on ENDF/B-VI [17] and were incorporated in the *cinder.dat* file, while the neutron spectrum was taken from the ^{235}U ACE library. Later, the gamma bin-wise data was augmented with ENDF/B-VI line data which was incorporated into the *cindergl.dat* file. In late 2008, release of the next-generation delayed-neutron emission data [18] sparked the creation of a new delayed-particle database, called *delay_library.dat*. As discussed below, this database has since been populated with the latest ENDF/B-VII delayed-beta and delayed-gamma emission data.

2.4. Sampling Algorithms

MCNP6 delayed-particle sampling algorithms come in two forms: bin-based (i.e., using bin-wise data) and line-based sampling. In general, line-based sampling is more exact; however it almost always comes with a significant penalty in execution speed. Details regarding these sampling techniques can be found in reference 7. Unless stated otherwise, subsequent discussions are associated with bin-based integration and sampling.

3. PHYSICS AND ALGORITHM ENHANCEMENTS

During this past year, three significant improvements have been made to the MCNP6 delayed-particle physics package. Discussions and results for each of these are provided in the following sections. The test problems presented in these sections were run using the first-collision option, which includes transport of source particles to only the first collision and transport of secondary particles unattenuated to the tally surface (see the 8th entry on the LCA card in reference 19).

3.1. Delayed-beta Feature

The emission of delayed betas from activation and fission is an important component of background signals produced from radiation sources, such as those proposed for active interrogation. The theory and implementation details for this capability follow that prescribed for bin-wise delayed-gamma production in MCNPX [7,9]. In its current form, this approach accumulates independent time and energy distributions of delayed-beta emission based on a CINDER90 decay-chain analysis for a specified residual. In the case of fission, this evaluation is performed twice – once for each of the two sampled fission products (see discussion above for details regarding neutron and photon-induced fission-product distributions). While the accumulation of these energy and time distributions can be time-consuming, this process is performed only once for each precursor or residual.

The MCNP6 *delay_library.dat* file has been updated to include bin-wise delayed-beta spectra for 957 nuclides, using a 100-keV bin structure (i.e., 100 bins from 0 to 10 MeV). The current data was taken from line and continuum data contained in the ENDF/B-VII Decay Data Sublibrary. A second larger version of the *delay_library.dat* file provides a 10-keV bin structure for this data.

The new MCNP6 delayed-beta feature is controlled using the *FISSION* and *NONFISS* keywords associated with the ACT card (see reference 19). The “e” particle type can be listed as an option for these keywords, which by default include only “n” and “p” for *FISSION* (i.e., delayed

neutrons and gammas from fission) and "none" for *NONFISS* (i.e., no delayed particles from activation).

In this first example, 12-MeV neutrons are incident on ^{16}O, resulting in the occasional production of ^{16}N via the [n,p] reaction. Fig. 1a presents the delayed-beta spectrum from this reaction, and Fig. 1b gives the related time distribution of the emitted betas. In this case, 0.026 betas were produced per collision, which corresponds to ~1 beta per [n,p] reaction. The ^{16}N discrete beta energies are apparent in Fig. 1a, and the time distribution in Fig. 1b is consistent with the ^{16}N seven-second half-life.

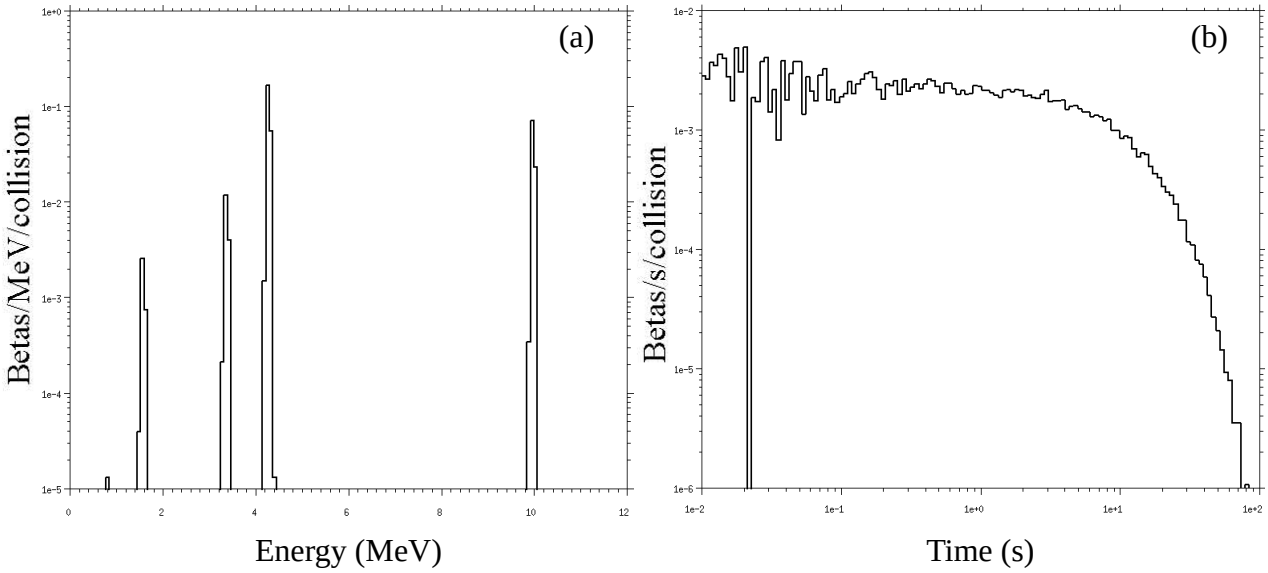

Figure 1. Beta spectrum and time distribution from 12-MeV neutrons incident on ^{16}O.

In the next example, thermal neutrons are incident on ^{136}Xe, resulting in the occasional production of ^{137}Xe, which then decays to ^{137}Cs and ^{137m}Ba. Fig. 2a provides the corresponding beta spectrum, where the high-energy peaks are produced by ^{137}Xe, the mid-energy peaks (~0.5-1.0 MeV) are produced by ^{137}Cs, and the low-energy peaks are produced by ^{137m}Ba. The integral number of emitted betas is 0.6 per collision, or ~3 betas per ^{137}Xe produced. In this case, the time distribution is a bit more complicated, involving the half-life of all three unstable nuclei (see Fig. 2b).

The final example involves thermal neutron fission of ^{235}U. In this case ~1300 fission products are produced, most of which have decay chains involving one or more daughter nuclei. Fig. 3a presents the resulting beta spectrum, which contains numerous beta emission lines, and Fig. 3b gives the corresponding time distribution.

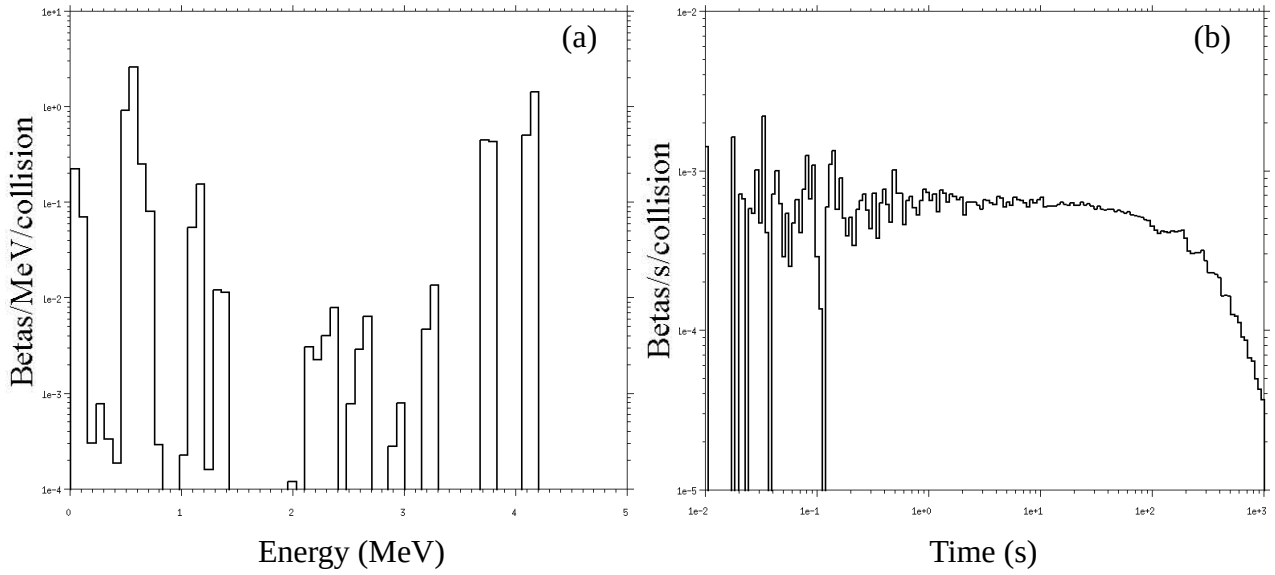

Figure 2. Beta spectrum and time distribution from thermal neutrons incident on ^{136}Xe.

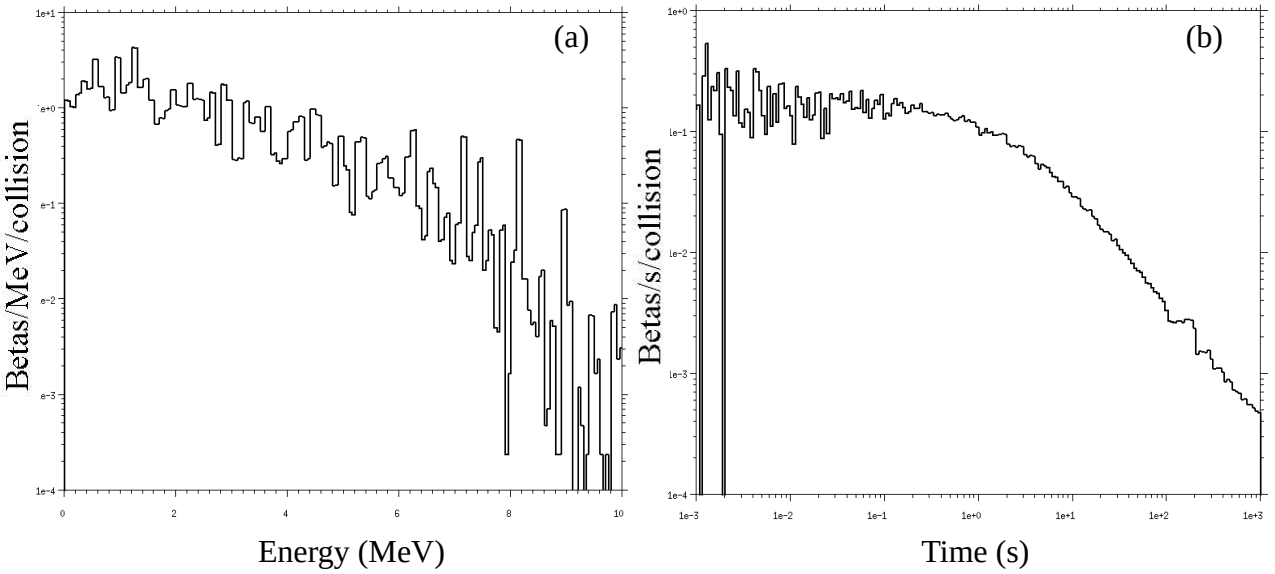

Figure 3. Beta spectrum and time distribution from thermal fission of ^{235}U.

3.2. Delayed-neutron Algorithm Enhancement

The delayed-neutron feature, last upgraded in MCNPX in 2009, has been enhanced again to fully account for all delayed-neutron emission within a decay chain (see the *FISSION=n* and *DN=model* options of the ACT card). Previously, the delayed-neutron spectrum was taken from only the precursor nuclide, while the time distribution included contributions from all nuclei

within a decay chain. With this enhancement, both the spectrum and time distributions include contributions from all daughter nuclei.

In the first example, 30-MeV neutrons are incident on ^{137}Te. At this high energy, neutrons frequently undergo inelastic scatter that results in the production of ^{137}Te and its daughter ^{137}I, each of which have a slightly different delayed-neutron spectrum. Fig. 4 gives a comparison of the old spectrum (blue), which includes only ^{137}Te, and the new spectrum (black), which is a combination of the two nuclei. Fig. 5 presents the time distribution of the delayed-neutron emission and indicates that the old and new treatments are consistent in their time-dependent behavior (i.e., the time integration already included contributions from all decay products).

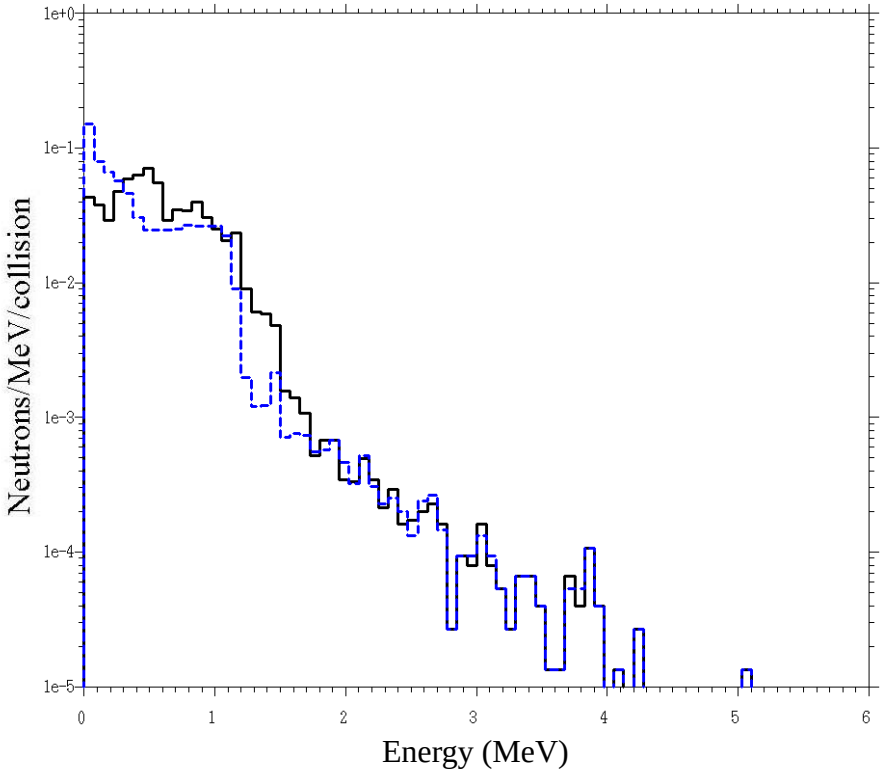

Figure 4. Delayed-neutron energy spectrum from 30-MeV neutrons incident on ^{137}Te.

In the last delayed-neutron example, 1-MeV neutrons are incident into ^{17}C. For some interactions, the [n,n′γ] reaction occurs, producing a ^{17}C residual, and for others the [n,2n] reaction occurs, producing a ^{16}C residual. Fig. 6 provides a comparison of the delayed-neutron spectrum for the old (blue) and new (black) treatments. In both cases, there is a mixture of the ^{16}C and ^{17}C delayed-neutron emission lines, but in the latter case there are also lines related to the decay of ^{17}C into ^{17}N. As in the previous example, the time distribution for both treatments remains unchanged (see Fig. 7 – the blue and black curves overlap each other).

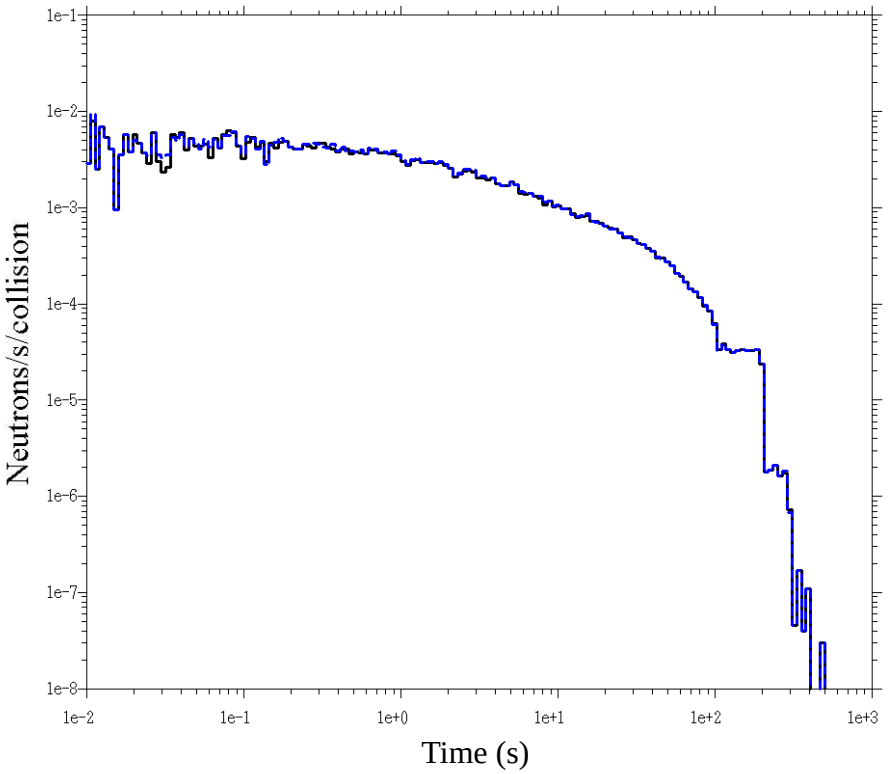

Figure 5. Delayed-neutron time distribution from 30-MeV neutrons incident on ^{137}Te.

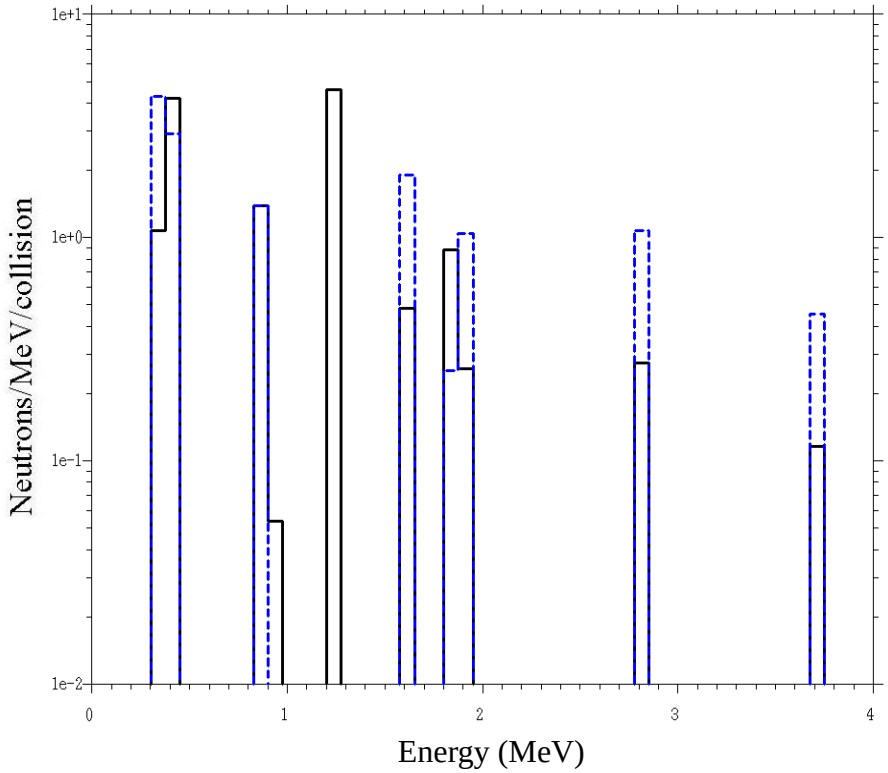

Figure 6. Delayed-neutron energy spectrum from 1-MeV neutrons incident on ^{17}C.

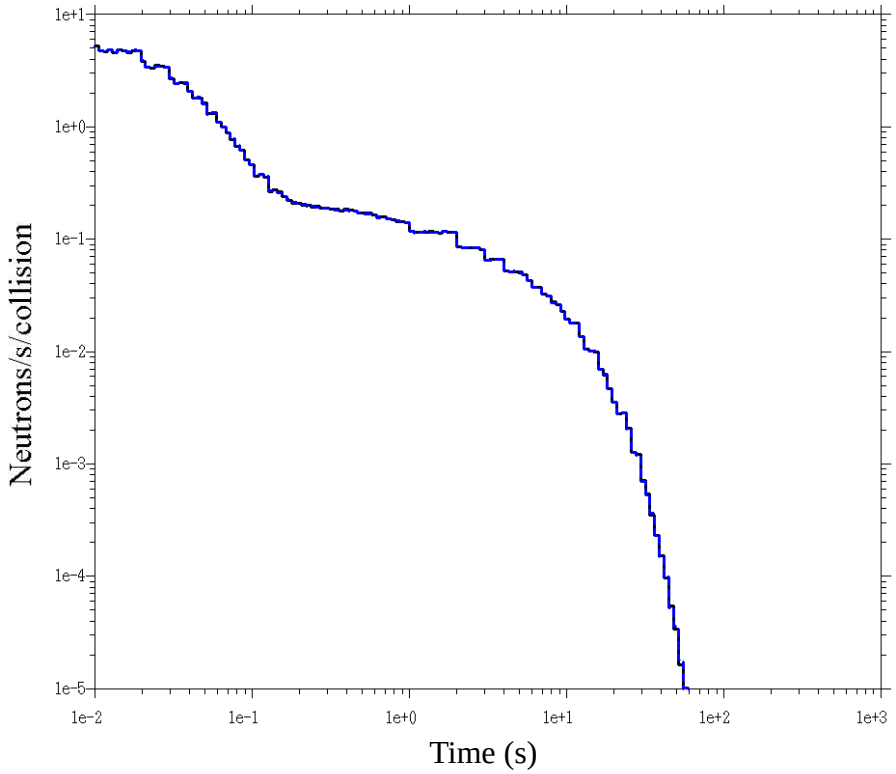

Figure 7. Delayed-neutron time distribution from 1-MeV neutrons incident on ^{17}C.

3.3. Delayed-gamma Database Enhancement

The bin-wise delayed-gamma feature in MCNP6 has been enhanced to utilize a refined bin structure and updated emission data (see the *DG=mg* option on the ACT card). Previously, a non-uniform 10-1000 keV bin structure was used (25 bins), and the emission data was based on ENDF/B-VI evaluations. With this delayed-gamma database enhancement, the bin structure has been refined (uniform 10 keV) and the emission data has been updated to ENDF/B-VII. As with the delayed-beta and delayed-neutron data, this data was incorporated into the *delay_library.dat* file.

In the final example, 1-eV neutrons are incident into ^{235}U, with the option to emit delayed gammas from fission only (i.e., *FISSION=p* and *NONFISS=none* options). Fig. 8 presents the delayed-gamma spectrum, summed over all fission products, for the old (blue, 25 bins) and new (black, 1000 bins) treatments. Also shown in this figure (red), is the delayed-gamma spectrum produced by the MCNP6 very-high-fidelity line treatment (i.e., *DG=line* option), which executes nearly 2 times slower than the new bin-wise treatment (1000 bins). Integral values for these spectra are 9.0 γ/f (old treatment), 6.0 γ/f (new treatment), and 6.5 γ/f (line treatment). These latter two are more in line with values found in the literature [20].

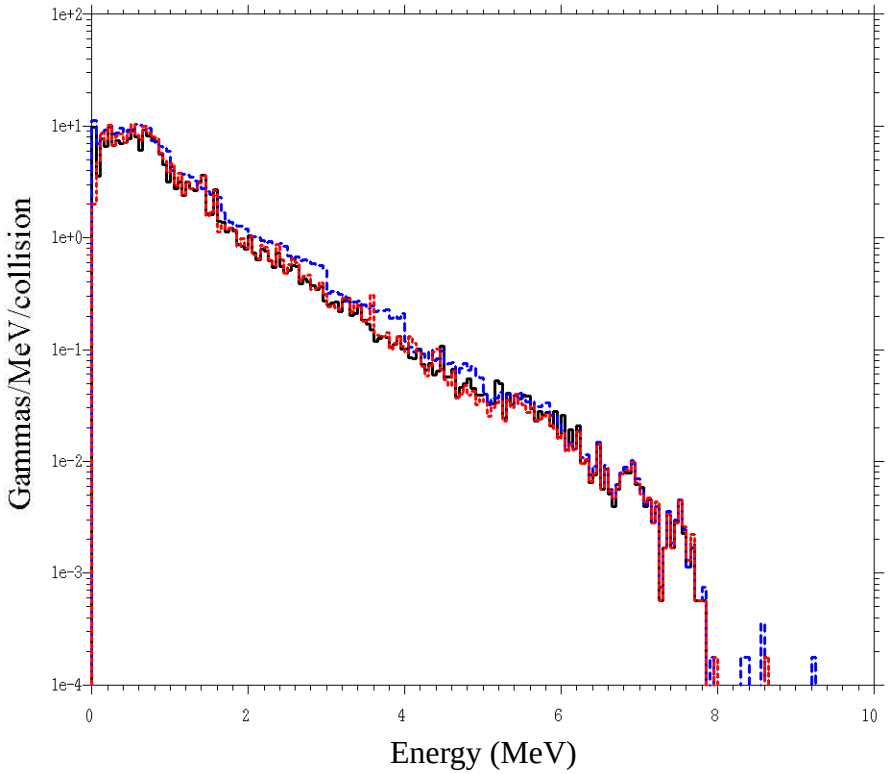

Figure 8. Delayed-gamma energy spectrum from neutron fission of ^{235}U.

4. CONCLUSIONS

Three significant enhancements have been made to the MCNP6 delayed-particle physics package, including the development of a delayed-beta capability, an algorithm enhancement for the delayed-neutron treatment, and a database enhancement for delayed-gamma emission. Results from test problems are shown for each of these enhancements, and these serve to demonstrate and verify these new capabilities. Combined, these improvements provide MCNP6 with a flexible state-of-the-art physics package for generating high-fidelity delayed signatures from fission and activation.

ACKNOWLEDGMENTS

We gratefully acknowledge the sponsorship of DHS/DNDO for this work.

REFERENCES

1. J. Pruet, J. Hall, M. Descalle, and S. Prussin, “Monte Carlo Models for the Production of β-Delayed Gamma-rays Following Fission of Special Nuclear Materials,” *Nuclear Instruments and Methods in Physics Research B*, **222**, pp. 403-410 (2004).
2. G. Weidenspointner, M. Harris, S. Sturner, and B. Teegarden, “MGGPOD: a Monte Carlo Suite for Modeling Instrumental Line and Continuum Backgrounds in Gamma-ray Astronomy,” *The Astrophysical Journal Supplement Series*, **156**, pp. 69-91 (2005).

3. J. Klingensmith and I. Gauld, “ORIGEN-S Gamma Decay Spectra Characterization and Benchmarking,” *Transactions of the American Nuclear Society*, **93**, pp. 33-34 (2005).
4. H. Trellue and G. McKinney, “Transmutation Feature within MCNPX,” *Proceedings of the MCNEG Conference*, Teddington, UK, March 15-18 (2004).
5. W. Wilson, T. England, D. George, D. Muir, and P. Young, “Recent Development of the CINDER90 Transmutation Code and Data Library for Actinide Transmutation Studies,” Los Alamos National Laboratory Report LA-UR-95-2181 (1995).
6. D. Pelowitz, editor, “MCNPX User’s Manual, Version 2.5.0,” Los Alamos National Laboratory Report LA-CP-05-0369 (2005).
7. J. Durkee, M. James, G. McKinney, H. Trellue, L. Waters, and W. Wilson, “Delayed-gamma Signature Calculation for Neutron-induced Fission and Activation Using MCNPX, Part I: Theory,” *Progress in Nuclear Energy*, **51**, pp. 813-827 (2009).
8. J. Durkee, M. James, G. McKinney, H. Trellue, L. Waters, and W. Wilson, “Delayed-gamma Signature Calculation for Neutron-induced Fission and Activation Using MCNPX, Part II: Simulations,” *Progress in Nuclear Energy*, **51**, pp. 828-836 (2009).
9. J. Durkee, M. James, G. McKinney, H. Trellue, L. Waters, and W. Wilson, “Delayed-gamma Signature Calculation for Neutron-induced Fission and Activation Using MCNPX, Part III: Transport Theory,” *Progress in Nuclear Energy*, **51**, pp. 837-844 (2009).
10. D. Pelowitz, editor, “MCNPX User’s Manual, Version 2.6.0,” Los Alamos National Laboratory Report LA-CP-07-1473 (2008).
11. F. Brown et al., “MCNP – A General Monte Carlo N-Particle Transport Code, Version 5 – Volume 1 Overview and Theory,” Los Alamos National Laboratory Report LA-CP-03-1987 (2003).
12. D. Pelowitz, editor, “MCNP – A General Monte Carlo N-Particle Transport Code, Version 6 – Volume 1 Overview and Theory,” Los Alamos National Laboratory Report LA-CP-11-xxxx, in print (2011).
13. M. Chadwick, P. Oblozinsky, M. Herman et al., “ENDF/B-VII.0: Next Generation Evaluated Nuclear Data Library for Nuclear Science and Technology,” *Nuclear Data Sheets*, **107**, pp. 2931-3060 (2006).
14. T. England and B. Rider, “Evaluation and Compilation of Fission Product Yields,” Los Alamos National Laboratory Report LA-UR-94-3106 (1994).
15. K. Schmidt and B. Jurado, “General Model Description of Fission Observables,” Le Centre d-Etudes Nucleaires de Bordeaux Gradignan CNRS/IN2P3 Report (2010).
16. R. Keepin, T. Wimett, and R. Zeigler, “Delayed Neutrons from Fissionable Isotopes of Uranium, Plutonium, and Thorium,” Los Alamos National Laboratory Report LA-02118 (1957).
17. V. McLane et al., “ENDF-201 ENDF/B-VI Summary Documentation Supplement I, ENDF/HE-VI Summary Documentation,” Brookhaven National Laboratory Report BNL-NCS-17541 (1996).
18. T. Kawano, P. Moller, and W. Wilson, “Calculation of Delayed-Neutron Energy Spectra in a Quasiparticle Random-Phase Approximation – Hauser-Feshbach Model,” *Phys. Rev. C*, **78**, 054601 (2008).
19. D. Pelowitz, editor, “MCNPX User’s Manual, Version 2.7.0,” Los Alamos National Laboratory Report LA-CP-11-0438 (2011).
20. T. Gozani, “Fission Signatures for Nuclear Material Detection,” *IEEE Transactions on Nuclear Science*, **56**, pp. 736-741 (2009).